Appendix

1.1 MR Image Acquisition Parameters

Each protocol included T1-weighted pre- and post-contrast images (T1 and T1C, respectively), T2-weighted fluid-attenuated inversion recovery images (FLAIR), and diffusion weighted images (DWI). Image acquisition was performed on our institutional MRI scanners, including 1.5T and 3T GE (General Electric Health, Waukesha, Wisconsin) and Siemens magnets (Siemens Healthineers, Erlangen, Germany). Example acquisition parameters for scans collected at 1.5T include (repetition time/echo time): T1 spin-echo sequence (T1), 666/14 ms; contrast-enhanced T1 acquired with gadolinium (T1C), 666/14 ms; apparent diffusion coefficient (ADC), calculated from diffusion-weighted images (DWI) acquired with a spin-echo echo-planar sequence, 10,000/90.7 ms; and FLAIR, acquired with an inversion recovery sequence, 10,000/151.8 ms and TI of 2,200 ms. Example acquisition parameters for scans collected at 3T include: T1 spin-echo sequence, 716.7/10 ms, T1C 716.7/10 ms, ADC from DWI acquired with a spin-echo echo-planar sequence, 8,000/83.1 ms, and FLAIR acquired with an inversion recovery sequence, 10,000/121.1 ms. All images were acquired with submillimeter in-plane resolution and a slice thickness between 3-6.5 mm.

1.2 Ex-vivo Tissue Processing

At autopsy, each patient's brain was removed and placed in a patient-specific 3D-printed brain mold, modeled from the patient's most recent MRI using surface renderings in 3D Slicer (https://www.slicer.org/). These molds were meant to prevent tissue distortion during the 2 to 3 weeks of fixation in formalin[15,17,36]. Following fixation, brains were sliced using patient-specific slicing jigs, 3D modeled using Blender 2.75 (https://www.blender.org/), to ensure brain slicing in line with the axial slice orientation from the most recent MRI[17]. All 3D printing was

performed using a MakerBot Replicator Z18. Tissue samples measuring approximately 2 inches by 3 inches were then collected from each subject from regions of suspected tumor, as well as tissue adjacent to the suspected tumor region. These samples were then processed, embedded in paraffin, sliced, and stained with hematoxylin and eosin (H&E). The slides were then digitized at 0.2 microns per pixel (40X magnification) using a Huron sliding stage microscope.

1.3 MRI-Histology Co-registration

The goal of this technique is to provide radio-pathomic alignments that account for shrinkage and deformation resulting from the various stages of tissue processing and provide for robust comparisons between imaging and histopathology[41,42]. This is achieved by first identifying the MRI slice that best corresponds to the tissue sample using photographs taken during tissue sectioning at autopsy. Next, a minimum of 20 control points were manually placed at corresponding points on the digital histology and the FLAIR image to identify anatomical landmarks and grey/white matter borders shared between the modalities. These landmarks are then used to compute a nonlinear warping that stretches the digital histology and its calculated features to match the MRI. Following visual quality assessment of the alignment, regions of interest (ROIs) were manually drawn to exclude areas where comparisons between the digital histology and MRI were not valid (i.e., tears or folds in the histology, ringing artifacts on the MRI).

Supplemental Figures

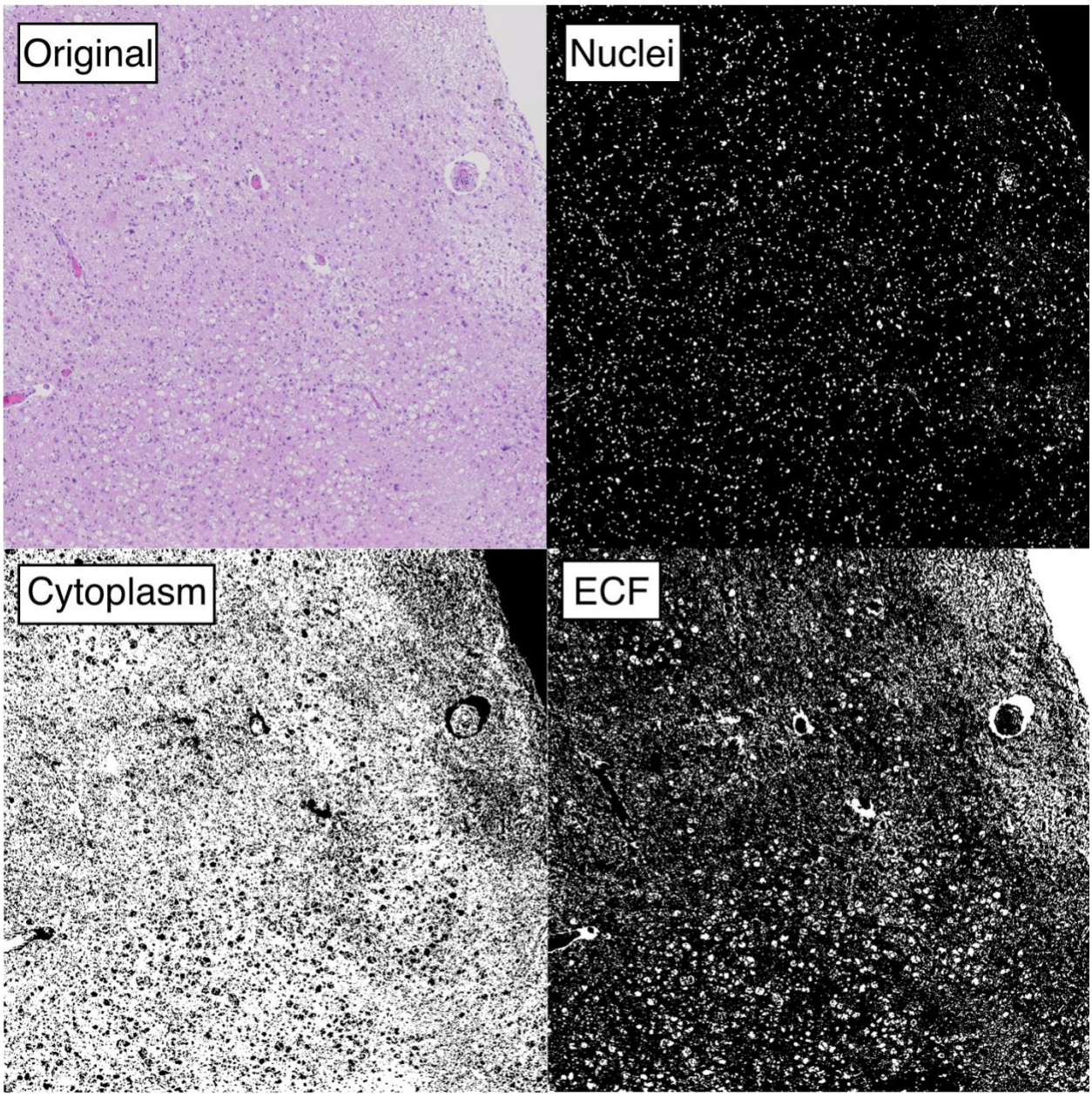

Supplemental Figure 1: Example tissue segmentations for a representative area of digitized tissue. Segmentations include nuclei (used for computing cell count), cytoplasm, and extracellular fluid (ECF).

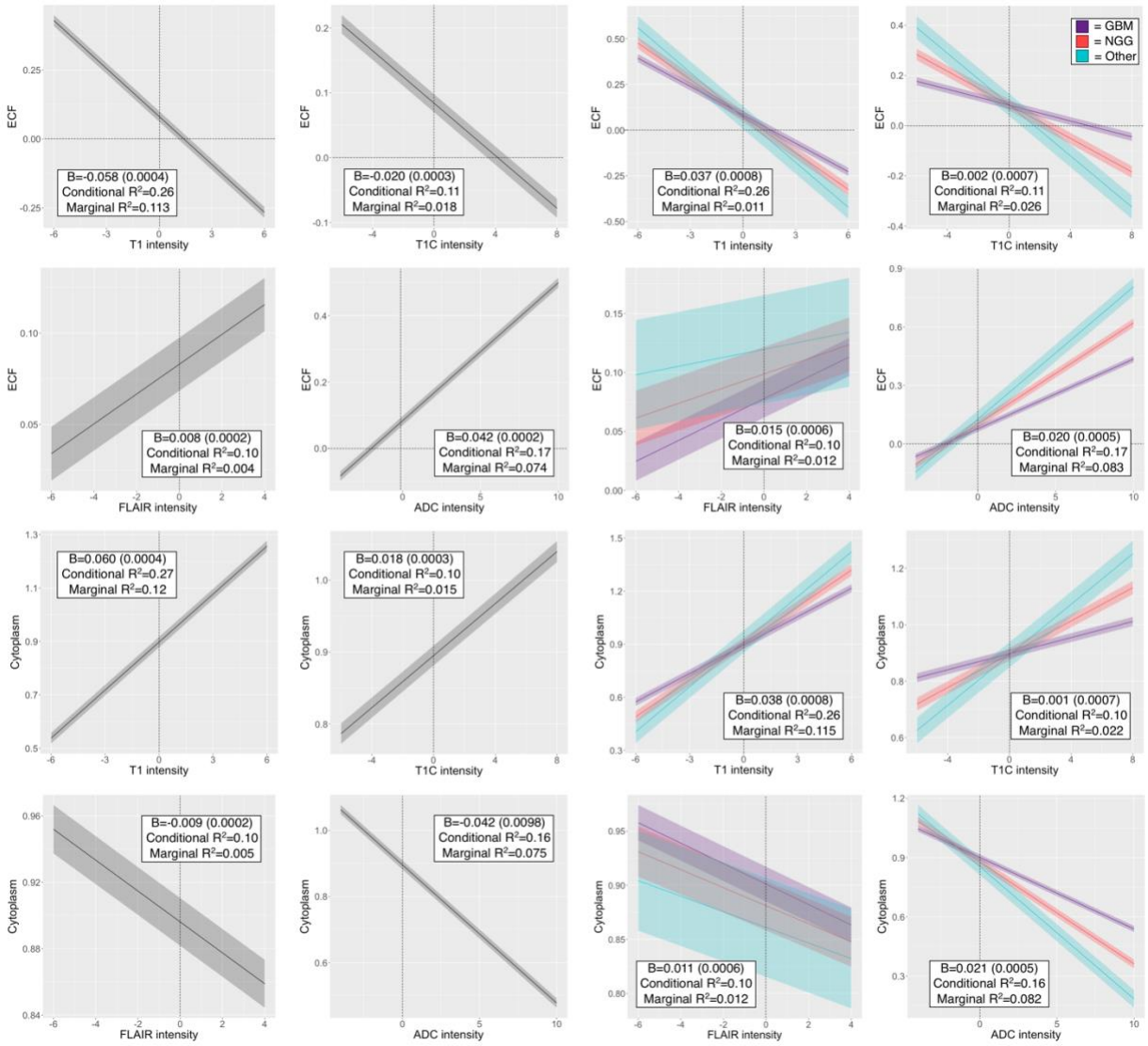

Supplemental Figure 2: Single image results depicting the relationship between image intensity and ECF/cytoplasm proportion for each contrast. B values for the left-hand plots indicate the change in ECF/cytoplasm proportion per standard deviation increase in image intensity. B values for the right-hand plots indicate the difference in slope between GBM, NGG, and Other patients.

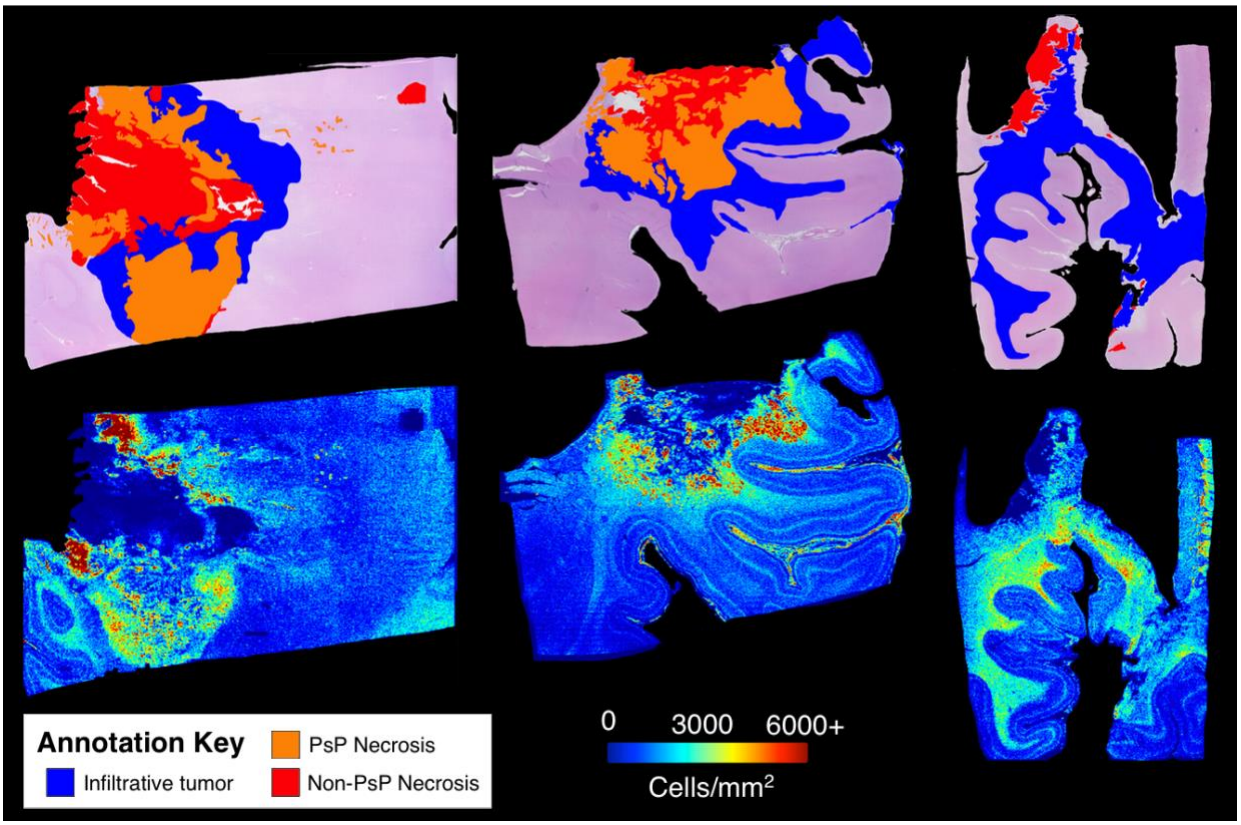

Supplemental Figure 3: Cellularity segmentations compared to representative pathological annotations for a subset of autopsy tissue samples. Cellularity segmentations tend to estimate areas of hypercellularity that closely follow annotations for tumor pathology (infiltrative tumor and pseudopalisading (PsP) necrosis), while correctly showing reduced cellularity in the presence of non-tumor necrosis.